Stability of anisotropic beams with space charge

I. Hofmann
GSI Darmstadt, Planckstrasse 1, 64291 Darmstadt, Germany
(Received 21 October 1997)

Based on self-consistent Vlasov-Poisson equations, we derive coherent frequencies and stability properties of anisotropic or ''nonequipartitioned'' beams with different focusing constants and emittances in the two transverse directions. The thus obtained dispersion relations of transverse multipole oscillations with quadrupolar, sextupolar, and octupolar symmetries are solved numerically. We find that for sufficiently large energy anisotropy some of the eigenmodes become unstable in the space-charge-dominated regime. Applying our results to high-current linear accelerators, we find that ''nonequipartitioned'' beams may exist in relatively large regions of parameter space under stable conditions. It is only in beams with strongly space-charge-depressed betatron tunes that harmful instabilities leading to emittance exchange should be expected.
[S1063-651X(98)01704-8]

PACS number(s): 41.75.−i, 29.27.Bd, 29.17.+w, 52.25.Wz

I. INTRODUCTION

Coupling resonances leading to an exchange of energy between different degrees of freedom are a familiar subject in accelerators. It is usually assumed that they are driven by first or higher order deviations from ideal linear focusing. In this paper we show that in the space-charge-dominated regime beam self-fields can play a similar role in coupling and lead to truly two-dimensional behavior, which differs significantly from that of beams where the two degrees of freedom are treated symmetrically (isotropic beams). We find that in the presence of internal energy anisotropy initially small space-charge-coupling terms can grow exponentially due to collective instability for sufficiently strong space-charge effects. For weak space charge as in circular accelerators, the coherent frequencies calculated here allow us to determine coherent shifts of sum or difference linear or nonlinear resonances up to fourth order. We note that energy anisotropy can result from different emittances as well as focusing strengths.

The subject has a potential application in present studies of high-current linear accelerators for protons or ions like spallation neutron sources, radioactive waste transmutation linacs, or heavy ion fusion linacs. In linac bunches one of the crucial beam dynamics issues is to what extent deviations from ''equipartitioning'' (equal average oscillation energy in all degrees of freedom) can be tolerated without risk of emittance growth (see Refs. [1,2] for some recent discussions). Anisotropy leading to collective instability in the presence of space charge was suggested in Ref. [3] as a possible approach to the equipartitioning question, since collisions cannot be made responsible for energy transfer in linacs due to their—relatively—short length. Although our mathematical model is constrained to anisotropy between the two transverse directions of a long beam—the only case where a self-consistent analysis seems possible—we suggest that the same mechanism of instability and similar thresholds are responsible for the longitudinal-transverse coupling in linac bunches. For the different problem of an infinitely long beam with initially zero longitudinal momentum spread but finite transverse emittance, an analytical study was presented in Ref. [4]; in a recent computer simulation of this problem it was found that possibly a similar mechanism is responsible for coupling [5]. The work of Refs. [4,5] was based on freely propagating waves in the direction of infinite beam extent, which is the main difference with our model of a confined beam.

A further potential application of the theory developed here are beam halos. It is assumed that mismatch oscillations can drive particles into a halo as a result of resonant interaction of these particles with the mismatch mode [6]. So far only second order (envelope oscillations) round (isotropic) beams have been considered as possible mismatch modes; the influence of anisotropy on second and higher order mismatch modes is expected to be an important factor in halo formation.

The theory presented here might also be relevant to the field of longitudinal laser cooling of bunched ion beams in storage rings. Recent experiments have shown that bunches close to the longitudinal space-charge limit can be achieved [7]. We expect that for sufficiently high intensity the anisotropy instability leads to an exchange of transverse and longitudinal oscillation energies, and thus enforces a collective indirect cooling of the transverse degrees of freedom.

The mechanism of collisionless coherent anisotropy instabilities discussed here has an analogy in infinite plasmas confined by magnetic fields. Temperature anisotropy in such plasmas can give rise to electrostatic instabilities, which remove the anisotropy [8,9]. Beams are essentially different due to the presence of an external focusing potential, which leads to the finite transverse dimension and changes the eigenmode structure substantially.

It should be mentioned that our analysis contains as a special case the eigenmodes of round isotropic beams in constant focusing which were derived earlier [10] for the Kapchinskij-Vladimirskij (KV, or δ function) distribution [11]. While results for the isotropic case can be expressed in terms of one dimensionless parameter ν/ν_0, anisotropy requires two further dimensionless parameters, for instance, the ratio of betatron frequencies and the ellipticity in real space.

The paper is organized in the following way: We start in

Sec. II with the equilibrium phase space distribution; in Secs. III and IV we solve Vlasov's equation and the resulting dispersion relations, whereas Sec. V presents applications to coherent tune shift and to the equipartitioning concept.

II. BASIC EQUATIONS

The unperturbed equilibrium beam is assumed to have uniform density within an elliptic cross section defined by

$$\left(\frac{x}{a}\right)^2+\left(\frac{y}{b}\right)^2\leqslant 1\,, \tag{1}$$

with a and b the semiaxes of the confining ellipse. In the longitudinal direction the beam is supposed to be uniform. From Poisson's equation one obtains the well-known expression for the space-charge electric field inside a beam of particles with charge q and line density N $(=n\pi ab)$ in free space:

$$E_x=-\frac{qNx}{\epsilon_0\pi a(a+b)},\qquad E_y=-\frac{qNy}{\epsilon_0\pi b(a+b)}. \tag{2}$$

Assuming linear and time-independent external focusing forces for the equilibrium beam (''smooth approximation'') we can write separate Hamiltonians for the x and y motions:

$$H_{0x}=(p_x^2+m^2\gamma^2\nu_x^2x^2)/(2m\gamma),\qquad H_{0y}=(p_y^2+m^2\gamma^2\nu_y^2y^2)/(2m\gamma); \tag{3}$$

and corresponding single-particle equations of motion as

$$\dot{p}_x=-m\gamma\nu_x^2x,\quad \dot{x}=p_x/(m\gamma),\qquad \dot{p}_y=-m\gamma\nu_y^2y,\quad \dot{y}=p_y/(m\gamma). \tag{4}$$

ν_{0x} and ν_{0y} are the betatron frequencies without space charge. The reduced betatron frequencies in the presence of space charge are conveniently expressed as

$$\nu_x^2=\nu_{0x}^2-\omega_p^2/(1+a/b),\qquad \nu_y^2=\nu_{0y}^2-\omega_p^2/(1+b/a), \tag{5}$$

where we have introduced the ''beam plasma frequency'' in the laboratory frame according to

$$\omega_p^2=\frac{q^2N}{\epsilon_0\pi m\gamma^3ab}. \tag{6}$$

The assumption of uniform density is consistent with a δ-function distribution of a linear combination of the two separate Hamiltonians which is a generalization of the Kapchinskij-Vladimirskij distribution

$$f_0(x,y,p_x,p_y)=\frac{NT\nu_y/\nu_x}{2\pi^2m\gamma a^2}\,\delta(H_{0x}+TH_{0y}-m\gamma\nu_x^2a^2/2). \tag{7}$$

Here T is the ratio of oscillation energies in the x and y directions which can be readily written for harmonic oscillators as

$$T=\frac{a^2\nu_x^2}{b^2\nu_y^2}. \tag{8}$$

The ratio of emittances is given by

$$\frac{\epsilon_x}{\epsilon_y}=\frac{a^2\nu_x}{b^2\nu_y}. \tag{9}$$

The time-independent f_0 in Eq. (7) is a solution of Vlasov's equation

$$\frac{df}{dt}\equiv\frac{\partial f}{\partial t}+\dot{x}\frac{\partial f}{\partial x}+\dot{y}\frac{\partial f}{\partial y}+\dot{p}_x\frac{\partial f}{\partial p_x}+\dot{p}_y\frac{\partial f}{\partial p_y}=0\,, \tag{10}$$

since H_{0x} and H_{0y} are constants of the motion. Integration over momentum space readily yields the uniform density within the boundary of Eq. (1).

For the perturbed distribution function $f\equiv f_0(H_{0x},H_{0y})+f_1(x,y,p_x,p_y,t)$, we linearize Vlasov's equation (see Ref. [12]), keeping only first-order terms in f_1 and in the perturbed electrostatic potential Φ, and obtain

$$\frac{df_1}{dt}\equiv\frac{\partial f_1}{\partial t}+\frac{p_x}{m\gamma}\frac{\partial f_1}{\partial x}+\frac{p_y}{m\gamma}\frac{\partial f_1}{\partial y}-m\gamma\nu_x^2x\frac{\partial f_1}{\partial p_x}-m\gamma\nu_y^2y\frac{\partial f_1}{\partial p_y}$$
$$=\frac{NTq\,\nu_y/\nu_x}{2\pi^2m^2\gamma^4a^2}\left(p_x\frac{\partial\Phi}{\partial x}+Tp_y\frac{\partial\Phi}{\partial y}\right)\times\delta'[p_x^2+\nu_x^2x^2+T(p_y^2+\nu_y^2y^2)-\nu_x^2a^2]. \tag{11}$$

The perturbed electrostatic potential Φ is self-consistently calculated by writing Poisson's equation for the perturbed charge density:

$$\nabla^2\Phi=-\frac{q}{\epsilon_0}n_1=-\frac{q}{\epsilon_0}\int f_1dp_xdp_y\,. \tag{12}$$

Equations (11) and (12) are a closed set of equations, which can be solved with an appropriate boundary condition for the electric field. Assuming that the beam pipe is sufficiently far away we can ignore image charges and take the boundary condition of an electric field vanishing at infinity.

III. INTEGRATION OF VLASOV'S EQUATION

In order to solve the coupled partial differential equations Eqs. (11) and (12), we use the method of characteristics by integrating df_1/dt along the unperturbed orbits. To this end we rewrite the solutions of the harmonic oscillator equations [Eqs. (4)] by introducing a phase angle $\varphi\equiv\nu_xt$ such that for $t'=t$ $(\varphi'=\varphi)$ the orbit goes through the point x,y,p_x,p_y in phase space:

$$
\begin{aligned}
x'(t') &= \frac{p_x}{\nu_x}\sin(\varphi'-\varphi)+x\,\cos(\varphi'-\varphi),\\
p_x'(t') &= p_x\cos(\varphi'-\varphi)-x\nu_x\,\sin(\varphi'-\varphi),\\
y'(t') &= \frac{p_y}{\nu_y}\sin[\alpha(\varphi'-\varphi)]+y\,\cos[\alpha(\varphi'-\varphi)],\\
p_y'(t') &= p_y\cos[\alpha(\varphi'-\varphi)]-y\nu_y\sin[\alpha(\varphi'-\varphi)].
\end{aligned}
\tag{13}
$$

Here we have introduced the ratio of betatron frequencies $\alpha\equiv\nu_y/\nu_x$. We now assume that α is rational, hence

$$
\alpha=\frac{n}{m},
\tag{14}
$$

with n and m some integer numbers. In this case the orbit given by Eq. (13) is exactly periodic in φ' with period $L=2\pi m$. The perturbed distribution function along the unperturbed orbit, $f_1(t,\varphi)$, is then also periodic in φ, and the total derivative in Eq. (11) can be written in terms of two variables only:

$$
\frac{df_1}{dt}=\frac{\partial f_1}{\partial t}+\nu_x\frac{\partial f_1}{\partial\varphi}.
\tag{15}
$$

We note that the assumption of rational α is not a real restriction in the present context: there are always rational numbers arbitrarily close to any real number, hence for any finite time interval the deviation of the harmonic oscillator orbits of Eqs. (13) for rational α from the real orbit can be made arbitrarily small.

We can now assume an explicit time dependence for a single eigenmode by introducing a coherent mode frequency ω,

$$
f_1=f_1(\varphi)e^{-i\omega t},\quad \Phi=\Phi(\varphi)e^{-i\omega t}.
\tag{16}
$$

$f_1(\varphi)$ can be determined by integrating the total derivative df_1/dt over a full period L of the unperturbed orbit (see, for example, Ref. [12]):

$$
\begin{aligned}
\int_\varphi^{\varphi+L}\frac{df_1}{dt'}d\varphi' &= -i\omega\int_\varphi^{\varphi+L}f_1(\varphi')e^{-i\omega\varphi'/\nu_x}d\varphi'\\
&\quad+\nu_x\int_\varphi^{\varphi+L}\frac{\partial f_1}{\partial\varphi'}e^{-i\omega\varphi'/\nu_x}d\varphi'\\
&= \nu_x f_1(\varphi)e^{-i\omega\varphi/\nu_x}(e^{-i\omega L/\nu_x}-1).
\end{aligned}
\tag{17}
$$

Hence, by inserting Eq. (15) into Eq. (17), introducing $u\equiv\varphi'-\varphi$, and dropping the explicit time dependence, we obtain

$$
\begin{aligned}
f_1(\varphi) &= \frac{NTq\nu_y/\nu_x^2}{2\pi^2m^2\gamma^4a^2}(e^{-i\omega L/\nu_x}-1)^{-1}\delta'\\
&\quad\times\int_0^L\left(p_x'\frac{\partial\Phi}{\partial x'}+Tp_y'\frac{\partial\Phi}{\partial y'}\right)e^{-i(\omega/\nu_x)u}du,
\end{aligned}
\tag{18}
$$

with, x', etc. according to Eqs. (13). After inserting f_1 into Eq. (12), we carry out the integration over the momentum space by introducing polar coordinates P and Θ according to $p_x=P\cos\Theta$ and $T^{1/2}p_y=P\sin\Theta$. Partial integration over P^2 leads to a nonvanishing boundary term for $P^2=0$ describing a surface charge perturbation on the unperturbed beam boundary, as well as a volume charge perturbation:

$$
\begin{aligned}
\nabla^2\Phi &= \frac{NT^{1/2}q^2\nu_y/\nu_x^2}{2\pi^2\epsilon_0m\gamma^3a^2}(e^{-2\pi im(\omega/\nu_x)}-1)^{-1}\\
&\quad\times\Bigg[2\pi\delta[m\gamma/2(\nu_x^2x^2+T\nu_y^2y^2-\nu_x^2a^2)]\\
&\quad\times\int_0^{2\pi m}e^{-i(\omega/\nu_x)u}\left(p_{x'}\frac{\partial\Phi}{\partial x'}+Tp_{y'}\frac{\partial\Phi}{\partial y'}\right)_{P^2=0}du\\
&\quad+2m\gamma\int_0^{2\pi m}e^{-i(\omega/\nu_x)u}\int_0^{2\pi}\frac{d}{dP^2}\left(p_{x'}\frac{\partial\Phi}{\partial x'}\right.\\
&\quad\left.+Tp_{y'}\frac{\partial\Phi}{\partial y'}\right)_{P^2=m^2\gamma^2(\nu_x^2(a^2-x^2)-T\nu_y^2y^2)}du\,d\Theta\Bigg].
\end{aligned}
\tag{19}
$$

It is straightforward to verify that—owing to the δ-function equilibrium distribution—the unknown solutions for Φ can be taken as finite order polynomials in x and y in the interior of the beam, matched to outside solutions that satisfy Laplace's equation in elliptic coordinates:

$$
\nabla^2\Phi=\frac{1}{c^2(\cosh^2\xi-\cos^2\varphi)}\left(\frac{\partial^2\Phi}{\partial\xi^2}+\frac{\partial^2\Phi}{\partial\varphi^2}\right)=0,
\tag{20}
$$

with

$$
\begin{aligned}
x &= c\,\cosh\xi\,\cos\,\varphi,\\
y &= c\,\sinh\,\xi\,\sin\,\varphi,\\
c^2 &= a^2-b^2.
\end{aligned}
\tag{21}
$$

Here we assume without loss of generality that $a\geqslant b$. The outside solution [$\xi>\xi_0$, with $\cosh\xi_0=a/c$)] is a superposition of angular harmonics which vanish at infinity:

$$
e^{-\ell(\xi-\xi_0)}\cos\ell\varphi,\quad e^{-\ell(\xi-\xi_0)}\sin\ell\varphi.
\tag{22}
$$

Integration of Eq. (19) across the beam boundary at $\xi=\xi_0$ gives rise to a jump of the derivative $\partial\Phi/\partial\xi$ that equals the surface charge on the boundary and matches the inside with the outside solution:

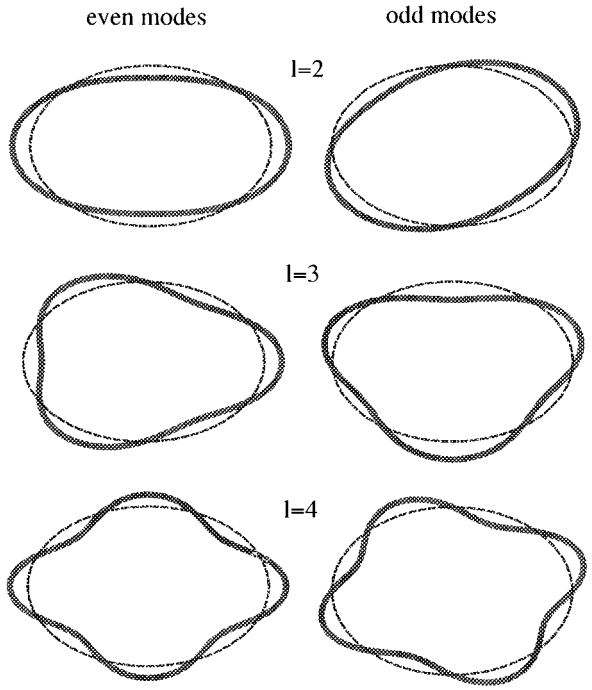

FIG. 1. Beam cross sections for second, third and fourth order even and odd modes (schematic, with x horizontal and y vertical coordinates).

$$\left[\frac{\partial\Phi}{\partial\xi}\right]_{\xi_0-0}^{\xi_0+0}=\frac{Nq^2/\nu_x^3}{\pi\epsilon_0 m^2\gamma^4 a^2}(e^{-2\pi i m(\omega/\nu_x)}-1)^{-1}\times\int_0^{2\pi m}e^{-i(\omega/\nu_x)u}\left(p_{x'}\frac{\partial\Phi}{\partial x'}+Tp_{y'}\frac{\partial\Phi}{\partial y'}\right)_{P^2=0}du. \tag{23}$$

IV. DISPERSION RELATION

The requirement of solving Eqs. (19) and (23) with a polynomial ansatz for Φ in the interior and the angular harmonic expansion Eq. (22) outside leads to a dispersion relation for the coherent frequency ω. It is a peculiarity of the δ-function distribution that only the leading terms in the x, y expansion of Φ are needed to determine the eigenfrequency. In the subsequent list of eigenfunctions we therefore ignore all lower order terms. Eigenmodes are characterized by the leading power l in this expansion, where we limit the evaluation to second, third, and fourth orders; furthermore they are characterized by the symmetry with respect to the angular variable φ, where the even modes $[\cos(l\varphi)]$ have the x axis as symmetry plane. The order l of this polynomial is related to the spatial profile of the density perturbation in the x,y plane as is shown in Fig. 1.

It is noted that the even modes are symmetric with respect to the horizontal (here x) axis. The odd modes lack this symmetry; in three dimensions these modes correspond to a lack of rotational symmetry around the longitudinal axis, hence they are suppressed in $r-z$ simulation codes. For rotationally symmetric unperturbed beams a distinction between even and odd modes is unnecessary, as is the case in Ref. [10]. For completeness we note that the first order modes corresponding to a rigid displacement of the beam are a trivial case. In the absence of image charges the corresponding coherent frequencies are just the zero-space-charge betatron frequencies in either direction.

By inserting the expanded Φ into Eqs. (19) and (23) we obtain linear equations for the expansion coefficients and find the dispersion relation in each order as condition of vanishing determinant. For convenience we introduce a set of three dimensionless variables to describe the equilibrium beam in terms of intensity, ratio of betatron frequencies and the envelope ratio (ellipticity):

$$\sigma_p^2\equiv\frac{\omega_p^2}{\nu_x^2},\quad \alpha\equiv\frac{\nu_y}{\nu_x},\quad \eta\equiv\frac{a}{b}(\geqslant 1). \tag{24}$$

The eigenfrequency is characterized by the dimensionless coherent frequency

$$\sigma\equiv\frac{\omega}{\nu_x}. \tag{25}$$

Hence the energy anisotropy is given by η^2/α^2 and the ratio of emittances by η^2/α. The dimensionless frequency depends on the three parameters σ_p^2,α, and η, where α is related to its zero intensity value α_0 according to

$$\alpha^2=\alpha_0^2+\frac{\sigma_p^2}{1+\eta}(\alpha_0^2-\eta). \tag{26}$$

A. Second order (envelope and tilting modes)

We begin with the even modes, which are the well-known envelope oscillations also following directly from the KV envelope equations [11] by linearizing them around the matched envelopes. The leading term in the perturbed space charge potential inside and outside for the even (e) mode is

$$\Phi_{2,e}^{(\mathrm{in})}=a_0x^2+a_2y^2,$$
$$\Phi_{2,e}^{(\mathrm{ex})}=\frac{a^2a_0}{2}+\frac{b^2a_2}{2}+\frac{(a^2a_0-b^2a_2)\cos(2\psi)}{2e^{2(\eta-\eta_0)}}, \tag{27}$$

and the dispersion relation results as

$$D_{2,e}\equiv(1+\eta)^2+\sigma_p^2\left(\frac{1+2\eta}{4-\sigma^2}+\frac{2\eta+\eta^2}{4\alpha^2-\sigma^2}\right)+\sigma_p^4\frac{2\eta}{(4-\sigma^2)(4\alpha^2-\sigma^2)}=0. \tag{28}$$

For the isotropic round beam with $\eta=1$ and $\alpha=1$, this reduces to

$$D_{2,e}\equiv 4+\frac{6\sigma_p^2}{4-\sigma^2}+\frac{2\sigma_p^4}{(4-\sigma^2)^2}, \tag{29}$$

which is solved by the familiar result

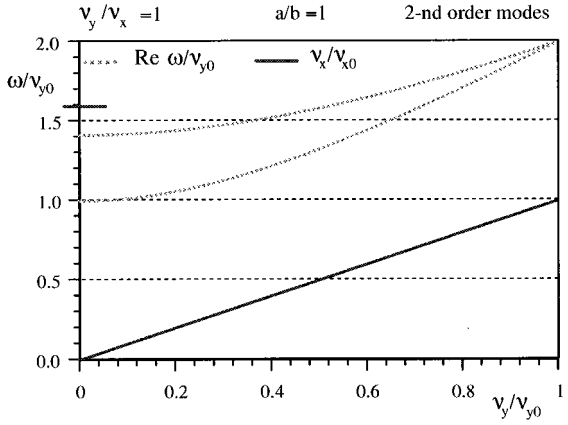

FIG. 2. Coherent frequencies of second order (envelope) modes for an isotropic round beam.

$$\sigma_1^2 = 4 + \sigma_p^2, \quad \sigma_2^2 = 4 + \frac{\sigma_p^2}{2}. \tag{30}$$

For zero space charge both mode frequencies approach the limiting frequency $\omega = 2\nu_0$ (ignoring the negative frequency branches). The high-frequency or ''fast mode'' corresponds to a round, spatially symmetric perturbation (''breathing mode''), and the low-frequency or''slow mode'' to a quadrupolar perturbation (spatially antisymmetric mode). The larger coherent tune shift of the breathing mode reflects the space-charge density compression. At the space-charge limit we obtain readily $\omega = \omega_p$ for the fast mode and $\omega = \omega_p/\sqrt{2}$ for the slow mode. It should be noted that in the anisotropic case both the fast and slow eigenmodes have quadrupolar symmetry.

The familiar results for envelope mode frequencies given in Eq. (30) are shown in Fig. 2. In this and the following graphs the eigenfrequencies have been normalized to ω/ν_{y0} and plotted against the ''tune depression'' ν_y/ν_{y0} for fixed ratio of betatron frequencies ν_y/ν_x and ellipticity a/b. This means that in the general anisotropic case according to Eq. (26) the ratio of external focusing constants, α_0, is not a constant in such a graph. We also plot the tune depression ν_x/ν_{x0}, which differs from ν_y/ν_{y0} in the general anisotropic case.

For the odd mode we have

$$\Phi_{2,o}^{(\mathrm{in})} = a_1 xy, \qquad \Phi_{2,o}^{(\mathrm{ex})} = \frac{aba_1 \sin(2\psi)}{2e^{2(\eta-\eta_0)}}, \tag{31}$$

which results in the dispersion relation

$$D_{2,o} \equiv (1+\eta)^2 + \frac{\sigma_p^2}{2}\left(\frac{(1-\alpha)(1-\eta^2/\alpha)}{(1-\alpha)^2-\sigma^2} + \frac{(1+\alpha)(1+\eta^2/\alpha)}{(1+\alpha)^2-\sigma^2}\right) = 0. \tag{32}$$

For the isotropic round case this simplifies to

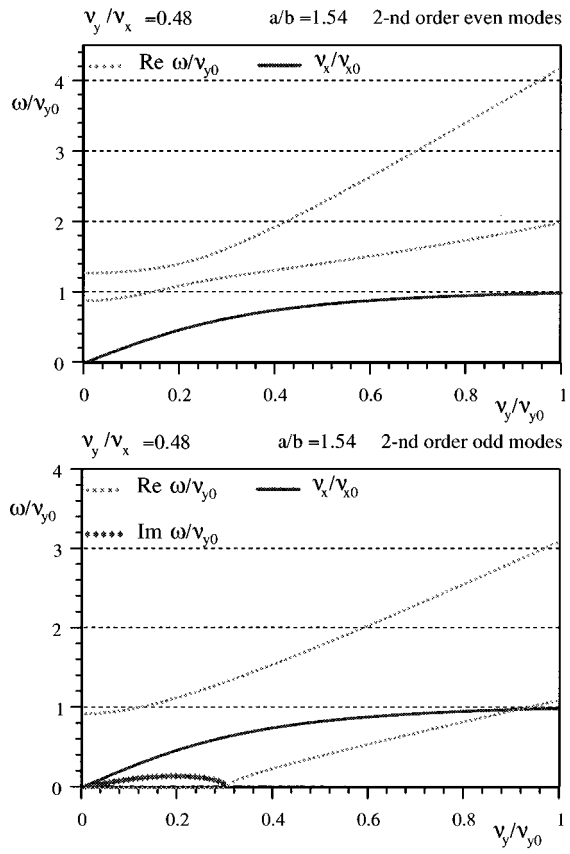

FIG. 3. Examples of coherent frequencies for second order even and odd modes for an anisotropic beam ($T = 10.5$).

$$D_{2,o} \equiv 4 + \frac{2\sigma_p^2}{4-\sigma^2}, \tag{33}$$

which is solved by $\sigma^2 = 4 + \sigma_p^2/2$. This is identical with the above even slow mode frequency, since for rotationally symmetric focusing the angular rotation has no restoring force. The odd slow frequency is zero for the same reason; it is only finite if the rotational symmetry is broken by unsymmetric focusing.

The solutions for the even mode are always stable, which is not necessarily true for the odd modes. We find that the low-frequency branch leads to imaginary ω if (assuming $\eta > 1$) the following conditions are satisfied :

$$\alpha < 1, \quad 1 < \alpha_0 < \sqrt{\eta}. \tag{34}$$

This means that the beam is unstable if for an external focusing stronger in the y direction space charge leads to a stronger x focusing. This tilting instability between x and y obviously requires a sufficiently large anisotropy.

An example with anisotropy ($T = 10.5$) is shown in Fig. 3. The low-frequency branch of the odd mode becomes unstable at tune depression below 0.3. The instability occurs as ''confluence'' of a positive frequency branch ω with $-\omega$ (not shown in the figures) merging into a pair of solutions with $\mathrm{Re}\,\omega = 0$ (''nonoscillatory'') and $\mathrm{Im}\,\omega > 0$ (unstable) and $\mathrm{Im}\,\omega < 0$ (damped). The free energy driving this instability obviously stems from the anisotropy. It is noted from

Eqs. (28) and (32) that for vanishing space charge ($\sigma_p \to 0$) the zeros of the denominators determine the limiting mode frequencies. Hence the low-frequency odd mode is related to a ''difference resonance'' $\omega = \nu_{x0} - \nu_{y0}$. In our model the driving term for this ''difference resonance'' is not a skew quadrupole as in synchrotrons, but the internal space-charge force caused by the exponentially growing initial ''tilting'' of the beam cross section. As for synchrotron difference resonances, we may expect that the effect of the instability is an exchange of emittance between x and y. The corresponding high-frequency branch is related to a ''sum resonance'' $\omega = \nu_{x0} + \nu_{y0}$. For the even modes the zero-space-charge limits are $2\nu_{x0}$ and $2\nu_{y0}$. An alternative approach describing even and odd second order modes by a matrix formalism was derived in Ref. [13], and applied to a stellarator field for high-current electron beam transport.

B. Third order (sextupolar modes)

For higher than second order the perturbed densities lead to nonlinear space-charge forces. For $\ell = 3$ these forces have the same expansion in x and y as the fields from sextupole magnets. The spatial boundaries of these modes are shown in Fig. 1. It is noted that even and odd modes can be interchanged by exchanging x and y, which is not the case in second and fourth orders.

Leading order terms in the perturbed space-charge potential are

$$\Phi_{3,e}^{(\mathrm{in})} = a_0 x^3 + a_2 x y^2, \tag{35}$$

$$\Phi_{3,e}^{(\mathrm{ex})} = \frac{(3a^3 a_0 + a b^2 a_2)\cos(\psi)}{4e^{\eta - \eta_0}} + \frac{(a^3 a_0 - a b^2 a_2)\cos(3\psi)}{4e^{3(\eta - \eta_0)}}.$$

The even mode dispersion relation is

$$\begin{aligned} D_{3,e} \equiv (1+\eta)^3 + \frac{\sigma_p^2}{8}\Bigg[& \frac{1-5\eta}{1-\sigma^2} + \frac{9+27\eta+24\eta^2}{9-\sigma^2} \\ & + \frac{(1-2\alpha)(1-2\eta^2/\alpha)(3+\eta)}{(1-2\alpha)^2-\sigma^2} \\ & + \frac{(1+2\alpha)(1+2\eta^2/\alpha)(3+\eta)}{(1+2\alpha)^2-\sigma^2}\Bigg] + \frac{\sigma_p^4}{8}\Bigg[\frac{-1}{(1-\sigma^2)^2} \\ & + \frac{3}{(1-\sigma^2)(9-\sigma^2)} + \frac{3(1-2\alpha)}{(9-\sigma^2)[(1-2\alpha)^2-\sigma^2]} \\ & + \frac{3(1+2\alpha)}{(9-\sigma^2)[(1+2\alpha)^2-\sigma^2]}\Bigg] = 0, \end{aligned} \tag{36}$$

which is simplified for the isotropic round beam to

$$D_{3,e} = 8 + \sigma_p^2 \frac{12}{9-\sigma^2} - \sigma_p^4 \frac{4\sigma^2(3-\sigma^2)}{(9-\sigma^2)^2(1-\sigma^2)^2}, \tag{37}$$

with solutions

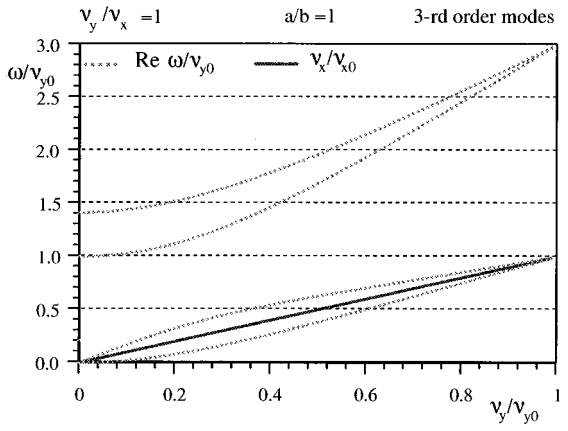

FIG. 4. Coherent frequencies of third order modes for an isotropic round beam.

$$\sigma_{1,2}^2 = \frac{10 + \sigma_p^2 \pm \sqrt{64 + 20\,\sigma_p^2 + \sigma_p^4}}{2},$$
$$\sigma_{3,4}^2 = \frac{20 + \sigma_p^2 \pm \sqrt{256 + 16\,\sigma_p^2 + \sigma_p^4}}{4}. \tag{38}$$

The numerical solutions for the coherent frequencies of the isotropic round case are shown in Fig. 4. As expected, no instability exists in this case [10].

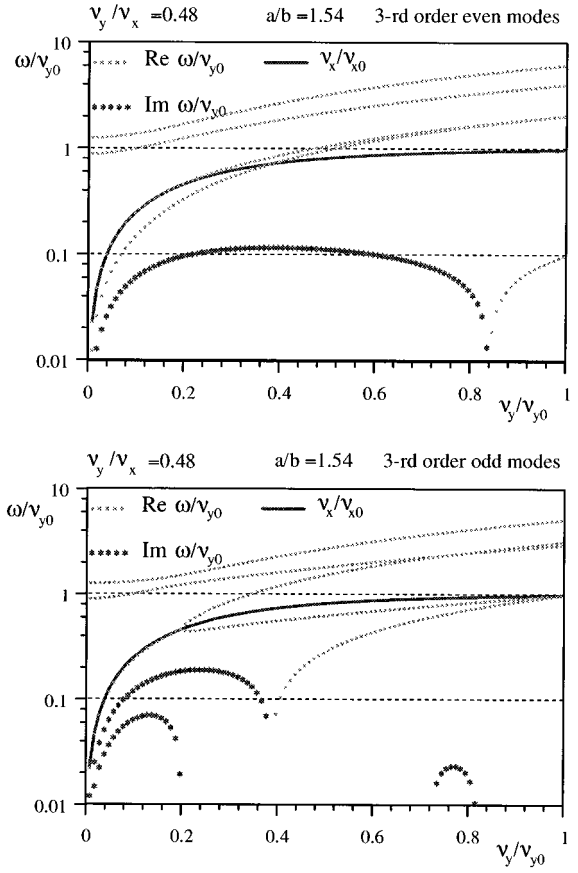

FIG. 5. Examples of coherent frequencies for third order even and odd modes for an anisotropic beam.

For the odd mode perturbed potential we have

$$\Phi_{3,o}^{(\mathrm{in})}=a_1x^2y+a_3y^3, \tag{39}$$

$$\Phi_{3,o}^{(\mathrm{ex})}=\frac{(a^2ba_1+3b^3a_3)\sin(\psi)}{4e^{\eta-\eta_0}}+\frac{(a^2ba_1-b^3a_3)\sin(3\psi)}{4e^{3(\eta-\eta_0)}}.$$

The odd mode dispersion relation is obtained by interchanging ν_x and ν_y as well as a and b in Eqs. (24) and (25), and solving Eq. (36) with the new variables. For an anisotropic case with the parameters of Fig. 3, the result is shown in Fig. 5.

For the anisotropic case we have chosen an example where instability appears below a critical tune depression. The first instability with Re $\omega=0$ (nonoscillatory) occurs for the even mode at $\nu_y/\nu_{y0}<0.84$ and for the odd mode at $\nu_y/\nu_{y0}<0.38$. The odd mode also shows oscillatory instability for $\nu_y/\nu_{y0}<0.2$ and a narrow band for $0.72<\nu_y/\nu_{y0}<0.81$. The normalized growth rates of the nonoscillatory case can be as large as 0.2, whereas the oscillatory growth rates are found to be much smaller (also see Sec. V B for details). The different branches in Fig. 5 can again be characterized by the resonant denominators of Eq. (36) and the corresponding odd mode expression.

C. Fourth order (octupolar modes)

Spatial boundaries of these modes have nonuniform density and space-charge forces like those of octupole magnets ($\ell=4$ in Fig. 1). For the perturbed even mode potentials

$$\Phi_{4,e}^{(\mathrm{in})}=a_0x^4+a_2x^2y^2+a_4y^4, \tag{40}$$

$$\Phi_{4,e}^{(\mathrm{ex})}=\frac{3\,a^4a_0+a^2b^2a_2+3\,b^4a_4}{8}+\frac{(a^4a_0-b^4a_4)\cos(2\,\psi)}{2e^{2(\eta-\eta_0)}}+\frac{(a^4a_0-a^2b^2a_2+b^4a_4)\cos(4\,\psi)}{8e^{4(\eta-\eta_0)}},$$

we find the dispersion relation

$$\begin{aligned}D_{4,e}\equiv{}&(1+\eta)^4+\sigma_p^2\left[\frac{5/4+5\,\eta+29\eta^2/4+4\,\eta^3}{(16-\sigma^2)}+\frac{3(1-\alpha)(1-\eta^2/\alpha)(1+4\,\eta+\eta^2)/8}{[4(1-\alpha)^2-\sigma^2]}\right.\\&+\frac{3(1+\alpha)(1+\eta^2/\alpha)(1+4\,\eta+\eta^2)/8}{[4\,(1+\alpha)^2-\sigma^2]}+\frac{4\,\eta+29\eta^2/4+5\,\eta^3+5\,\eta^4/4}{(16\,\alpha^2-\sigma^2)}-\frac{2\,\eta^2}{(4-\sigma^2)}-\left.\frac{2\,\eta^2}{(4\,\alpha^2-\sigma^2)}\right]-\sigma_p^4\left[\frac{1/4+\eta}{(4-\sigma^2)^2}\right.\\&-\frac{1/2+2\,\eta}{(16-\sigma^2)(4-\sigma^2)}-\frac{5\,\eta+9\,\eta^2+5\,\eta^3}{(16-\sigma^2)(16\alpha^2-\sigma^2)}+\frac{5\,\eta^2/2}{(4-\sigma^2)(16\alpha^2-\sigma^2)}+\frac{5\,\eta^2/2}{(16-\sigma^2)(4\alpha^2-\sigma^2)}-\frac{\eta^2/2}{(4-\sigma^2)(4\alpha^2-\sigma^2)}\\&+\frac{\eta^3+\eta^4/4}{(4\alpha^2-\sigma^2)^2}-\frac{2\,\eta^3+\eta^4/2}{(16\alpha^2-\sigma^2)(4\alpha^2-\sigma^2)}-\frac{3(1-\alpha)(1-\eta^2/\alpha)(1+4\,\eta)/8}{(16-\sigma^2)[4(1-\alpha)^2-\sigma^2]}-\frac{3(1+\alpha)(1+\eta^2/\alpha)(1+4\,\eta)/8}{(16-\sigma^2)[4(1+\alpha)^2-\sigma^2]}\\&-\left.\frac{3(1-\alpha)(1-\eta^2/\alpha)(4\,\eta+\eta^2)/8}{(16\alpha^2-\sigma^2)[4(1-\alpha)^2-\sigma^2]}-\frac{3(1+\alpha)(1+\eta^2/\alpha)(4\,\eta+\eta^2)/8}{(16\alpha^2-\sigma^2)[4(1+\alpha)^2-\sigma^2]}\right]+\sigma_p^6\left[\frac{-\eta}{(4-\sigma^2)^2(16\,\alpha^2-\sigma^2)}\right.\\&+\frac{2\,\eta}{(16-\sigma^2)(4-\sigma^2)(16\,\alpha^2-\sigma^2)}+\frac{3(1-\alpha)(1-\eta^2/\alpha)\,\eta/2}{(16-\sigma^2)[4\,(1-\alpha)^2-\sigma^2](16\,\alpha^2-\sigma^2)}\\&+\left.\frac{3(1+\alpha)(1+\eta^2/\alpha)\,\eta/2}{(16-\sigma^2)[4\,(1+\alpha)^2-\sigma^2](16\,\alpha^2-\sigma^2)}-\frac{\eta^3}{(16-\sigma^2)(4\,\alpha^2-\sigma^2)^2}+\frac{2\,\eta^3}{(16-\sigma^2)(16\,\alpha^2-\sigma^2)(4\alpha^2-\sigma^2)}\right]=0.\end{aligned} \tag{41}$$

For the round isotropic beam, this reduces to the expression

$$\begin{aligned}D_{4,e}\equiv{}&16+\sigma_p^2\left(\frac{44}{16-\sigma^2}-\frac{4}{4-\sigma^2}\right)+\sigma_p^4\left(\frac{-34}{(16-\sigma^2)^2}\right.\\&\left.+\frac{2}{(4-\sigma^2)^2}\right)+\sigma_p^6\left(\frac{6}{(16-\sigma^2)^3}-\frac{2}{(16-\sigma^2)(4-\sigma^2)^2}\right.\\&\left.+\frac{4}{(16-\sigma^2)^2(4-\sigma^2)}\right),\end{aligned} \tag{42}$$

with solutions

$$\sigma_1^2=16+\sigma_p^2,$$

$$\sigma_{2,3}^2=\frac{20+\sigma_p^2\pm\sqrt{(20+\sigma_p^2)^2-4\,(64-2\,\sigma_p^2)}}{2}. \tag{43}$$

$$\sigma_{4,5}^2=\frac{40+\sigma_p^2\pm\sqrt{(40+\sigma_p^2)^2-8\,(128+10\,\sigma_p^2)}}{4}$$

These coherent frequencies are shown in Fig. 6, which indicates an instability for $\nu/\nu_0<0.24$, which was identified in Ref. [10]. The origin of this instability is the δ-function nature of the initial distribution. It has been shown by means of computer simulation that this particular instability levels off at small amplitude with a practically negligable effect on the phase space density [16]. Analytical work has also shown that a moderate broadening of the δ-function distribution suffices to suppress this particular mode [15].

The odd modes have

$$\Phi_{4,o}^{(\mathrm{in})}=a_0x^3y+a_2xy^3,$$
$$\Phi_{4,o}^{(\mathrm{ex})}=\frac{(a^3ba_0+ab^3a_2)\sin(2\psi)}{4e^{2(\eta-\eta_0)}}+\frac{(a^3ba_0-ab^3a_2)\sin(4\psi)}{8e^{4(\eta-\eta_0)}} \tag{44}$$

and

$$\begin{aligned}
D_{4,o}\equiv{}&(1+\eta)^4+\frac{\sigma_p^2}{16}\left[\frac{2(1-\alpha)(1-\eta^2/\alpha)(1-4\eta+\eta^2)}{[(1-\alpha)^2-\sigma^2]}+2\frac{(1+\alpha)(1+\eta^2/\alpha)(1-4\eta+\eta^2)}{[(1+\alpha)^2-\sigma^2]}\right.\\
&+\frac{(1-3\alpha)(1-3\eta^2/\alpha)(5+4\eta+\eta^2)}{[(1-3\alpha)^2-\sigma^2]}+\frac{(1+3\alpha)(1+3\eta^2/\alpha)(5+4\eta+\eta^2)}{[(1+3\alpha)^2-\sigma^2]}\\
&\left.+\frac{(3-\alpha)(3-\eta^2/\alpha)(1+4\eta+5\eta^2)}{[(3-\alpha)^2-\sigma^2]}+\frac{(3+\alpha)(3+\eta^2/\alpha)(1+4\eta+5\eta^2)}{[(3+\alpha)^2-\sigma^2]}\right]\\
&+\frac{\sigma_p^4}{64}\left[-\frac{6(1-\alpha^2)(1-\eta^4/\alpha^2)}{[(1-\alpha)^2-\sigma^2][(1+\alpha)^2-\sigma^2]}-\frac{3(1-\alpha)^2(1-\eta^2/\alpha)^2}{[(1-\alpha)^2-\sigma^2]^2}-\frac{3(1+\alpha)^2(1+\eta^2/\alpha)^2}{[(1+\alpha)^2-\sigma^2]^2}\right.\\
&+\frac{(3-4\alpha+\alpha^2)(3-4\eta^2/\alpha+\eta^4/\alpha^2)}{[(1-\alpha)^2-\sigma^2][(3-\alpha)^2-\sigma^2]}+\frac{(3+4\alpha+\alpha^2)(3+4\eta^2/\alpha+\eta^4/\alpha^2)}{[(1+\alpha)^2-\sigma^2][(3+\alpha)^2-\sigma^2]}\\
&+\frac{(3-2\alpha-\alpha^2)(3-2\eta^2/\alpha-\eta^4/\alpha^2)}{[(1-\alpha)^2-\sigma^2][(3+\alpha)^2-\sigma^2]}+\frac{(3+2\alpha-\alpha^2)(3+2\eta^2/\alpha-\eta^4/\alpha^2)}{[(1+\alpha)^2-\sigma^2][(3-\alpha)^2-\sigma^2]}\\
&+\frac{(1+2\alpha-3\alpha^2)(1+2\eta^2/\alpha-3\eta^4/\alpha^2)}{[(1-\alpha)^2-\sigma^2][(1+3\alpha)^2-\sigma^2]}+\frac{(1-2\alpha-3\alpha^2)(1-2\eta^2/\alpha-3\eta^4/\alpha^2)}{[(1+\alpha)^2-\sigma^2][(1-3\alpha)^2-\sigma^2]}\\
&+\frac{(3+8\alpha-3\alpha^2)(3+8\eta^2/\alpha-3\eta^4/\alpha^2)}{[(3-\alpha)^2-\sigma^2][(1+3\alpha)^2-\sigma^2]}+\frac{(3-8\alpha-3\alpha^2)(3-8\eta^2/\alpha-3\eta^4/\alpha^2)}{[(3+\alpha)^2-\sigma^2][(1-3\alpha)^2-\sigma^2]}\\
&+\frac{(1+4\alpha+3\alpha^2)(1+4\eta^2/\alpha+3\eta^4/\alpha^2)}{[(1+\alpha)^2-\sigma^2][(1+3\alpha)^2-\sigma^2]}+\frac{(1-4\alpha+3\alpha^2)(1-4\eta^2/\alpha+3\eta^4/\alpha^2)}{[(1-\alpha)^2-\sigma^2][(1-3\alpha)^2-\sigma^2]}\\
&\left.+\frac{(3+10\alpha+3\alpha^2)(3+10\eta^2/\alpha+3\eta^4/\alpha^2)}{[(3+\alpha)^2-\sigma^2][(1+3\alpha)^2-\sigma^2)}+\frac{(3-10\alpha+3\alpha^2)(3-10\eta^2/\alpha+3\eta^4/\alpha^2)}{[(3-\alpha)^2-\sigma^2][(1-3\alpha)^2-\sigma^2)}\right]=0,
\end{aligned} \tag{45}$$

with the isotropic round beam limit

$$\begin{aligned}
D_{4,o}\equiv{}&16+\sigma_p^2\left(\frac{4}{4-\sigma^2}+\frac{20}{16-\sigma^2}\right)\\
&+\sigma_p^4\left(\frac{4}{(16-\sigma^2)^2}+\frac{4}{(16-\sigma^2)(4-\sigma^2)}\right).
\end{aligned} \tag{46}$$

The solutions are identical with the σ_1 and $\sigma_{4,5}$ of the even case due to the isotropy. In the anisotropic example of Fig. 7, we find a transition to nonoscillatory instability for $\nu_y/\nu_{y0}<0.3$, and several regions of oscillatory instability with smaller growth rates.

V. APPLICATIONS

A. Coherent tune shifts and resonances in circular machines

A potential application is the effect of transverse anisotropy and space charge in crossing of linear or nonlinear resonances in circular accelerators. The resonance condition $n\nu_{x0}+m\nu_{y0}=N$ (with n,m, and N integers, and ν_{x0} and ν_{y0}

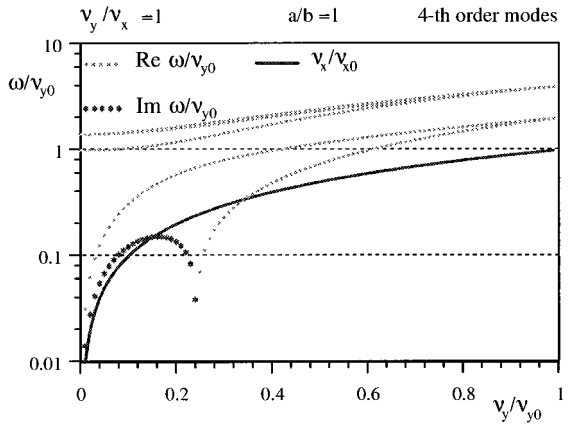

FIG. 6. Coherent frequencies of fourth order modes for an isotropic round beam.

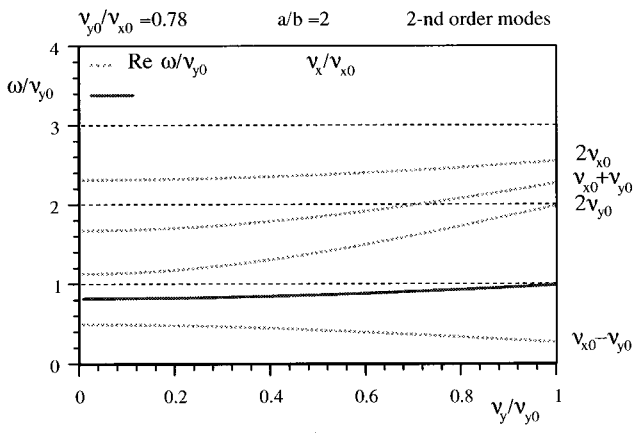

FIG. 8. Coherent tune shifts for sum, difference, and envelope resonances modified by space charge.

here defined as betatron tunes giving the number of betatron oscillation periods per revolution) defined in the absence of space charge cannot be replaced simply by using the space-charge-shifted incoherent betatron frequencies ν_x and ν_y since the ensemble of particles responds to the resonance in a coherent way. For such a coherently oscillating space charge the resonance condition is shifted, and should be replaced by the ''coherent resonance condition''

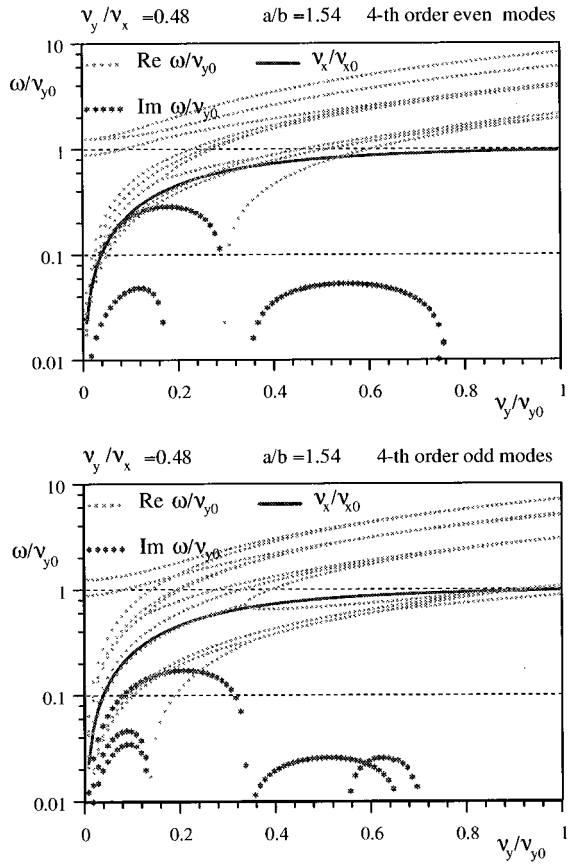

FIG. 7. Examples of coherent frequencies for fourth order even and odd modes for an anisotropic beam.

$$\omega = n\nu_x + m\nu_y + \Delta\omega = N, \tag{47}$$

which expresses the fact that the coherent mode resonates with the linear or nonlinear driving harmonic N.

In Fig. 8 we show the result for the coherent frequency of the linear (second order) resonance assuming a fixed ratio of the zero-space-charge betatron frequencies (here $\nu_{y0}/\nu_{x0} = 3.45/4.45 = 0.78$), hence the graph applies to a given focusing structure (in contrast with the graphs in Sec. IV). We characterize the modes according to their zero-space-charge frequencies: the odd modes which—in the presence of lattice skew quadrupole terms—lead to difference $(\nu_{x0} - \nu_{y0})$ or sum $(\nu_{x0} + \nu_{y0})$ resonances as well as the even modes $(2\nu_{x0}, 2\nu_{y0})$. Equations (28) and (32) can be used to determine the expected tune shifts.

B. Instability charts and equipartitioning

For the design of high-current linacs and other applications where stability is of interest it is desirable to identify regions in parameter space where growth rates leading to emittance exchange might occur. An important parameter

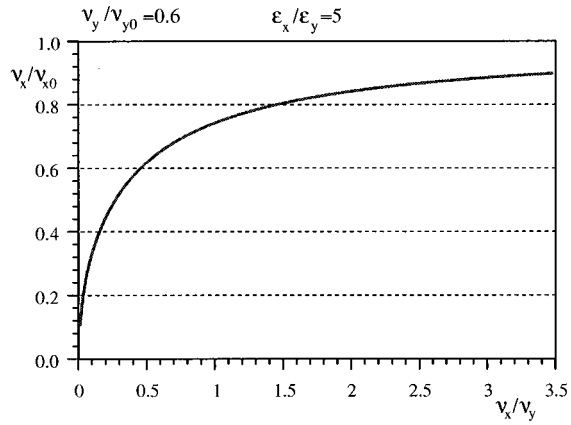

FIG. 9. Variation of the space-charge tune depression in x for a given emittance ratio and tune depression in y.

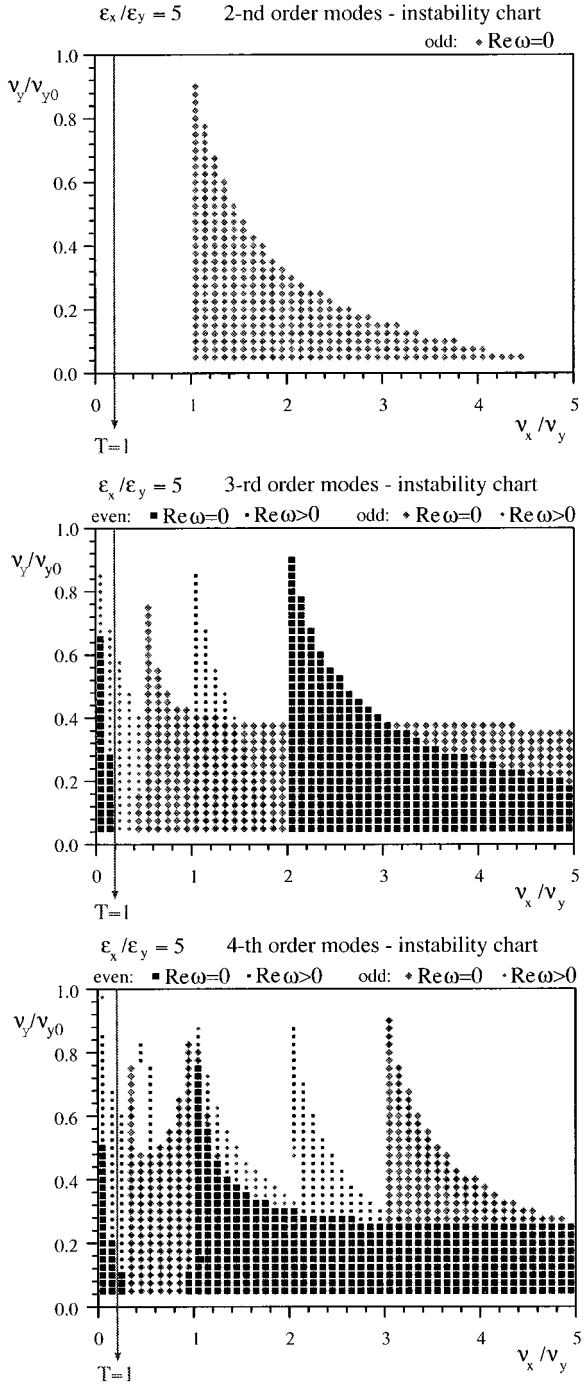

FIG. 10. Stability charts for second, third, and fourth order modes assuming $\epsilon_x/\epsilon_y=5$ (with square markers referring to even modes, and diamond markers to odd modes).

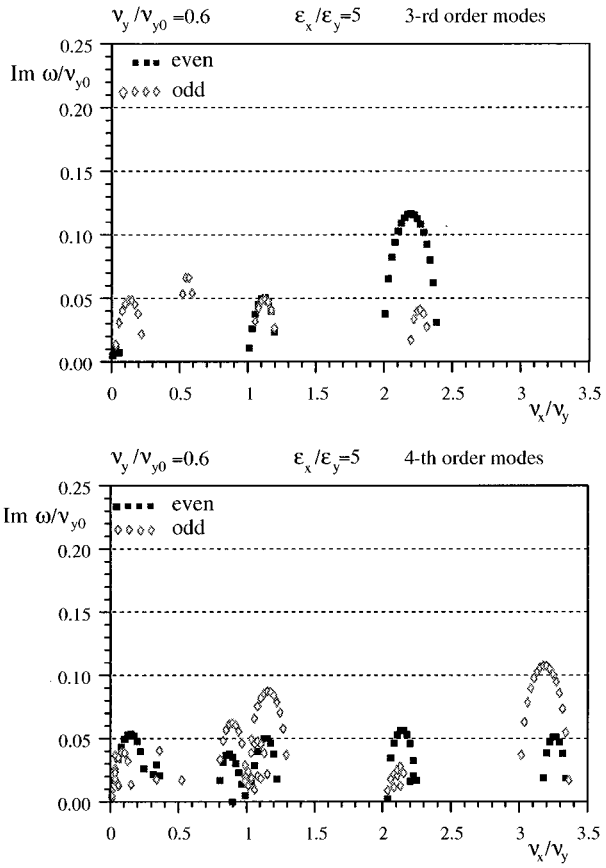

FIG. 11. Growth rates for constant $\nu_y/\nu_{y0}=0.6$ and $\epsilon_x/\epsilon_y=5$. Note that $T=1$ corresponds to $\nu_x/\nu_y=0.2$ on this graph.

besides anisotropy is the space-charge-induced tune depressions ν_y/ν_{y0} or ν_x/ν_{x0}. Since we use ν_y/ν_{y0} it should be kept in mind that the tune depression in x follows from the tune and emittance ratios. As an example, we show in Fig. 9 such a dependence for $\nu_y/\nu_{y0}=0.6$ and $\epsilon_x/\epsilon_y=5$. One finds that for $0<T<2.5$ ($0<\nu_x/\nu_y<0.5$) the x tune is the more strongly depressed one (only weakly dependent of the emittance ratio as long as $\epsilon_x/\epsilon_y \gg 1$).

In Fig. 10 we present charts which show the tune depression ν_y/ν_{y0} versus tune ratio for a given ratio of emittances, and corresponding marks whenever an eigenfrequency indicates instability. Hence, at the boundaries of the marked regions, growth rates vanish. The anisotropy T is given by the product of tune ratio and emittance ratio, and can be larger or smaller than unity. The largest growth rates are found for the nonoscillatory instabilities with $\mathrm{Re}\,\omega=0$ (large marks); for the oscillatory instabilities with $\mathrm{Re}\,\omega>0$ (small marks) growth rates are found to be generally smaller. Equipartitioning is indicated by the line $T=1$.

Regions of instability are found in a large fraction of parameter space. The practical significance of an unstable mode depends on the growth rate as well as the width of a zone of instability. Small bands of instability are easily left due to detuning by the changing emittance ratio, or by parameter changes during the acceleration process. In Fig. 11 we show the actual growth rates for cuts in Fig. 10 at $\nu_y/\nu_{y0}=0.6$, and in Fig. 12 at $\nu_y/\nu_{y0}=0.3$.

Large growth rates with extended bands are seen to occur only for the nonoscillatory modes with $\mathrm{Re}\,\omega=0$ and the stronger tune depression of 0.3. It is noteworthy that the unstable regions of these modes merge into the single-particle resonance conditions of difference resonances: $\nu_x-2\nu_y\approx 0$ and $2\nu_x-\nu_y\approx 0$ for the third order even and odd modes; and $2\nu_x-2\nu_y\approx 0$ and $\nu_x-3\nu_y\approx 0$, as well as $3\nu_x-\nu_y\approx 0$, for the fourth order even and odd modes. This suggests that these instabilities lead to emittance exchange between x and y.

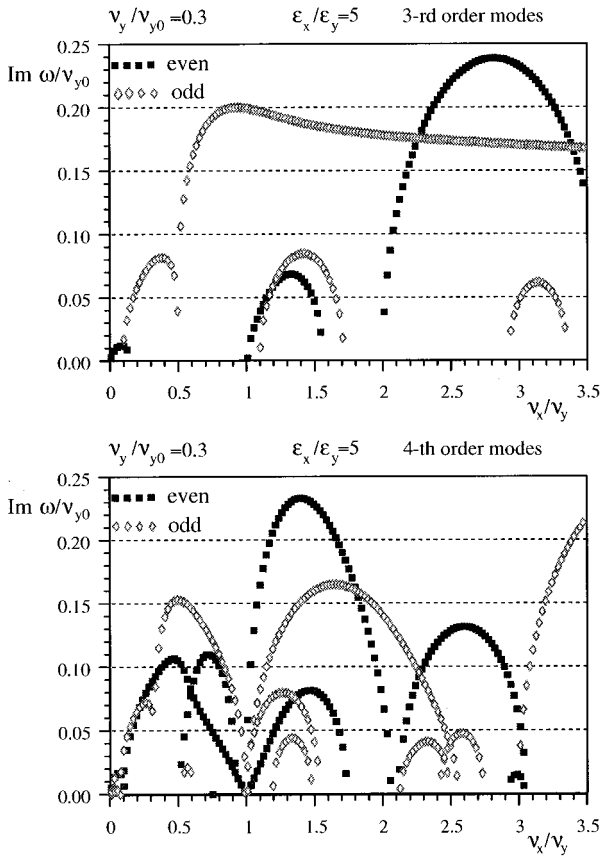

FIG. 12. Growth rates for constant $\nu_y/\nu_{y0}=0.3$ and $\epsilon_x/\epsilon_y=5$. Note that $T=1$ corresponds to $\nu_x/\nu_y=0.2$ on this graph.

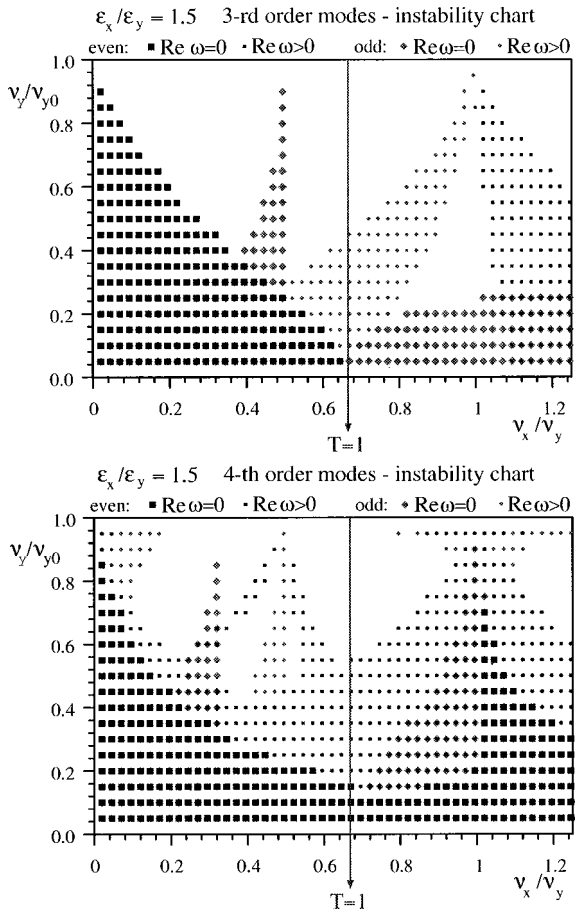

FIG. 13. Stability charts for third and fourth order modes assuming $\epsilon_x/\epsilon_y=1.5$ (with square markers referring to even, diamond markers to odd modes).

Linac design: With reference to the design of linear accelerators we suggest that these stability charts can give a useful orientation not only for the x-y coupling case but also for the more important longitudinal-transverse coupling (z-y and likewise z-x). If $\epsilon_l/\epsilon_t>1$ we identify l with x and t with y, whereas for $\epsilon_l/\epsilon_t<1$ one needs to identify l with y and t with x. Such a chart for a typical value of $\epsilon_x/\epsilon_y=1.5$ relevant to high-current linacs is shown in Fig. 13.

We find that there is sufficient space free of instabilities right and left of the equipartitioning line $T=1$. For $T=\frac{1}{3}$ (three times higher transverse oscillation energy), for instance, the transverse (y) tune depression must be below 0.6 (hence the longitudinal one is even significantly smaller according to Fig. 9) to enter into the unstable region of the third order (nonoscillatory) even mode, and even lower for the fourth order (nonoscillatory) even mode. This is hardly the case in any practical design, where one finds the transverse tune depression closer to 0.8. The oscillatory instabilities left of $T=1$ (see Figs. 11 and 12) have (normalized) growth rates limited to 0.05. This corresponds to the relatively long e-folding time of 20 periods of betatron oscillation (defined without space charge). The narrow spikes of odd mode instabilities near $\nu_x/\nu_y=0.5$ and $\nu_x/\nu_y=0.33$ are also expected to be harmless.

Growth rates inside the bands of instability as well as the width of these bands increase gradually if the transverse tune depression drops below 0.6, and if at the same time T is (sufficiently) above unity (or T sufficiently below unity if the emittance ratio is reversed). The normalized growth rates of 0.25 reached for the transverse tune depression of 0.3 (Fig. 12) would result in an e-folding time of four periods of betatron oscillation (defined without space charge). These are also, roughly speaking, the peak values of growth rates we have found for a variety of parameters.

Hence we conclude that linac beams can be ''nonequipartitioned'' without risk of emittance transfer, as long as the tune depression is not excessive. We suggest that the region of transverse tune depression between 0.7 and 1 should be safe from a practical point of view.

VI. CONCLUSION

We have shown that the step from one-dimensional to two-dimensional equilibria with anisotropy and space charge leads to considerably more complexity in the calculation of coherent tune shifts and in the stability behavior. Such beams must be described by three independent parameters. We argue that practically significant anisotropy instabilities occur for strong tune depression only, when extended regions in parameter space give instability predominantly of the nonoscillatory type. Hence, beams in ''nonequipartitioned''

linac designs with medium or weak space-charge tune depression can be expected to be stable and thus not subject to emittance exchange. Obviously computer simulation is required to take into account periodic focusing, external focusing nonlinearities, and the influence of more realistic distribution functions. The analytical theory may, however, serve as an important guideline in the multi-dimensional situation of real beams where the many free parameters make computer simulation extremely demanding.

ACKNOWLEDGMENTS

The author benefited from several discussions with R. A. Jameson and M. Reiser on the role of equipartitioning in linac design.

[1] R. A. Jameson, Fusion Eng. Des. **32–33**, 149 (1996).
[2] M. Reiser and N. Brown, Phys. Rev. Lett. **74**, 1111 (1995).
[3] I. Hofmann, IEEE Trans. Nucl. Sci. **NS-28**, 2399 (1981).
[4] T.-S. F. Wang and L. Smith, IEEE Trans. Nucl. Sci. **NS-28**, 2477 (1981).
[5] I. Haber, D. A. Callahan, A. Friedman, D. P. Grote, and A. B. Langdon, Fusion Eng. Des. **32–33**, 169 (1996).
[6] J. S. O'Connell, T. P. Wangler, R. S. Mills, and K. R. Crandall, in *Proceedings of the Particle Accelerator Conference* (The American Physical Society, Washington D.C., 1993), p. 3657.
[7] J. S. Hangst *et al.*, Phys. Rev. Lett. **74**, 4432 (1995).
[8] E. G. Harris, Phys. Rev. Lett. **2**, 34 (1959).
[9] E. G. Harris, J. Nucl. Energy C **2**, 38 (1961).
[10] R. L. Gluckstern, *Proceedings of the Linac Conference* (Fermilab, Batavia, 1970), p. 811.
[11] I. M. Kapchinskij and V. V. Vladimirskij, *Proceedings of the International Conference on High Energy Accelerators* (CERN, Geneva, 1959), p. 274.
[12] R. C. Davidson, *Methods in Nonlinear Plasma Theory* (Academic, New York, 1972), Chap. 4.
[13] D. Chernin, Part. Accel. **24**, 29 (1988).
[14] I. Hofmann, L. J. Laslett, L. Smith, and I. Haber, Part. Accel. **13**, 145 (1983).
[15] I. Hofmann, Phys. Fluids **23**, 196 (1980).